Structural reliability updating using monitoring data from in-situ load testing and laboratory test results

R. de Vries

Faculty of Civil Engineering and Geosciences, Delft University of Technology, Delft, The Netherlands Reliable Structures, Netherlands Organization for Applied Scientific Research (TNO), Delft, The Netherlands

E.O.L. Lantsoght

Faculty of Civil Engineering and Geosciences, Delft University of Technology, Delft, The Netherlands College of Sciences and Engineering, Universidad San Francisco de Quito (USFQ), Quito, Ecuador

R.D.J.M. Steenbergen

Reliable Structures, Netherlands Organization for Applied Scientific Research (TNO), Delft, The Netherlands

Faculty of Engineering and Architecture, Ghent University (UGent), Ghent, Belgium

M.A.N. Hendriks

Faculty of Civil Engineering and Geosciences, Delft University of Technology, Delft, The Netherlands Department of Structural Engineering, Norwegian University of Science and Technology (NTNU), Trondheim, Norway

M. Naaktgeboren

Rijkswaterstaat, Ministry of Infrastructure and Water Management, Utrecht, The Netherlands

ABSTRACT: Given the ageing infrastructure, verifying the reliability of existing structures is crucial. Field testing presents a viable approach to evaluating a structure's current condition, particularly proof load testing. In a proof load test, a large load is applied to assess its reliability. Structures in sound condition are expected to display satisfactory behaviour under average load intensities. Can good structural performance under moderate load levels already prove sufficient structural reliability? The proposed method utilises data from laboratory tests on similar structural elements. A case study was conducted on a bridge to illustrate the effectiveness of the method. Data acquired from laboratory tests were pre-processed to provide the required input for the reliability updating. It reveals that sufficient reliability can be demonstrated without excessive load levels by incorporating laboratory data. However, the actual capacity of the bridge and the uncertainty associated with the laboratory data remain important factors.

1 INTRODUCTION

Ensuring the reliability of bridges and viaducts is an ongoing effort involving inspections, structural assessments, and maintenance practices. As the infrastructure ages and experiences increased traffic loads and intensities, accurate assessment methods are required to account for the changing conditions. Load testing may be used to verify a bridge or viaduct's current structural integrity. A load test conducted to prove a structure's ability to withstand future traffic loads is referred to as a 'proof load test' (Alampalli et al., 2021; Faber et al., 2000; Lantsoght et al., 2017). The magnitude of the load to be applied in the test, commonly called the target load, is pivotal in proof load testing. If the structure can resist a large load without any

DOI: 10.1201/9781003483755-44

issues, it proves it is sufficiently reliable for future use. The magnitude of the target load is directly related to the reliability requirements. Often, such reliability requirements result in relatively large loads being applied to the structure (De Vries et al., 2023a). A potential solution to this problem is to probabilistically consider all relevant information about the structural resistance, especially the performance indicators during testing. Then, load testing can demonstrate the same reliability level with lower test loads, making it a cost-effective alternative to other evaluation methods.

The current article presents a novel reliability updating method that integrates information from two distinct sources: the survival of the applied load during the proof load test and the indicator value observed throughout the testing process. When a proof load test is conducted, the load is gradually applied in small steps until the target is reached to prevent unwanted damage. Measurement of displacements, crack widths and so on usually cannot instantly tell us about the structural performance. Therefore, corresponding stop criteria interpret the structural behaviour rather than the measurements directly (Zarate Garnica & Lantsoght, 2021). For example, strains may be interpreted via sectional analysis to identify a critical value. The type of expected damage and failure mechanism will define the specific stop criteria that should be used.

2 METHOD

2.1 Reliability updating using two information sources

When a particular load is resisted in a proof load test, the structure's resistance is at least equal to the load effect achieved during the test $(R \ge E_{\rm PL})$. The load effect consists of permanent loads and the load applied within the test $(E_{\rm PL} = G + Q_{\rm PL})$. This results in a truncation of the resistance distribution (Lin & Nowak, 1984). Naturally, there will be some uncertainty associated with this load effect. When accounted for, the truncation will be more gradual, still assigning some probability density to values lower than the intended (mean) proof load effect $(m_{E,\rm PL})$ (Brüske, 2018). This truncation results in the first source of information following from successfully withstanding the applied load (Figure 1, point 1).

The in-situ measurements and stop criteria introduced in the previous section are commonly used to prevent structural failure. The novel method described herein uses the measurement data to *predict* the structure's resistance at moderate load levels. This prediction gives rise to the second source of information following a load step in the proof load test. The prediction may be achieved using suitable data that links observed damage to the applied loading for similar structural elements. In this context, the measurements normally conducted within the application of stop criteria are called indicators. The strain calculated from displacement measurements at the bottom of a beam or slab is an example of such an indicator. From the data obtained in the

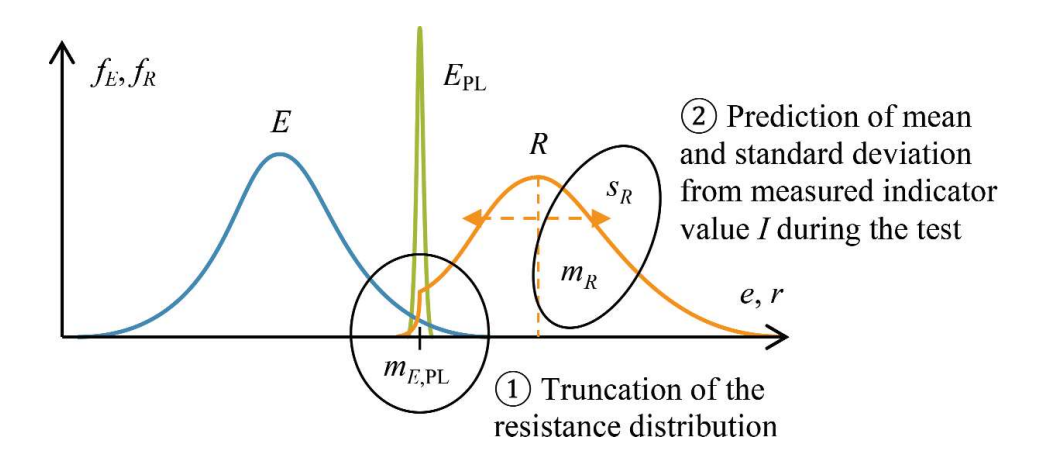


Figure 1. General principle of updating the resistance distribution from two sources of information.

laboratory tests and the indicator value observed during the in-situ test, the corresponding mean and standard deviation of the resistance may be inferred (Figure 1, point 2).

2.2 Probabilistic model for updating

The structural reliability is determined by evaluating a limit state function (Z), which results in a negative value when failure occurs. The limit state function for the assessment of a bridge (or viaduct) subjected to traffic load has been formulated in line with the Probabilistic Model Code (JCSS, 2015) and *fib* Bulletin 80 (fib, 2016):

$$Z = \theta_R R - \theta (G_{Dl} + G_{SDL} + C_{0Q} Q \tag{1}$$

where R is the resistance, θ_E is the model uncertainty of the load effect calculation, $G_{\rm DL}$ is the dead load, $G_{\rm SDL}$ is the superimposed dead load, C_{0Q} is the time-invariant part of the live load, and Q is the time-variant part of the live load. Here, θ_R accounts for the statistical model uncertainty in which in-situ testing is coupled with laboratory experiments. This uncertainty is small when the laboratory specimens are representative of the structure under consideration. However, large uncertainty should be expected if the structures are dissimilar or the measurement techniques and data post-processing differ. Real-world experience with the proposed method will give insight into appropriate model uncertainty values. The uncertainty in predicting the resistance from a measured indicator value will be contained in the ratio X and follows from the statistical processing of the laboratory data.

Each time the structure successfully resists a new load level, the distribution function of R may be updated to reflect the newly obtained information (Section 2.1). The updated distribution of R may be written as a multiplication of the ratio X and the load effect produced during the last successful load test cycle ($R = XE_{PL}$). Since the proof load is survived, this indicates $R \ge E_{PL}$ and therefore $X = R/E_{PL} \ge 1$. However, this does not imply that the resistance distribution is truncated at a fixed value because of the uncertainty in the proof load effect (E_{PL}) (Figure 1). The resulting distribution of R does not follow a regular distribution since it follows from the multiplication of X and E_{PL} , of which the latter is also a product of other random variables. The resistance R may be expanded and inserted into Equations (1), giving:

$$Z = \theta_R X [\theta_E (G_{DL} + G_{SDL}) + \theta_{E,PL}] - \theta_E (G_{DL} + G_{SDL} + C_{0Q}Q)$$
(2)

where $\theta_{E,\text{PL}}$ is the model uncertainty applicable for calculating the load effect from the applied proof load, and Q_{PL} is the load effect following from the applied load in the test. Because of the controlled conditions during the test, the uncertainty in calculating the load effect from the proof load is expected to be smaller than for the other loads. The calculation model and method will likely be the same for both; thus, a strong correlation exists between $\theta_{E,\text{PL}}$ and θ_{E} . For simplicity, it may be assumed that they are the same ($\theta_{E,\text{PL}} = \theta_{E}$), effectively eliminating them from the limit state equation:

$$Z = \theta_R X (G_{DL+} G_{SDL+} Q_{PL}) - (G_{DL} + G_{SDL} + C_{00} Q$$
(3)

Although the permanent loads $(G_{DL} + G_{SDL})$ appear in both the resistance and the load effect, they cannot be eliminated from the equation. Yet, it can be difficult to estimate them when the original drawings and calculations are lost or the structure has been modified. It is seen that the permanent load terms lead to an increase in the resistance since $X \ge 1$ must be satisfied to survive the proof load. Conservatively, the permanent load terms may be removed:

$$Z = \theta_R X Q_{\rm PL} - C_{0O} Q \tag{4}$$

For structures where the permanent loads are relatively small compared to the live load, Equations (4) results in similar reliability values as Equations (3). It may also be observed that with

X = 1, the lower bound approximation is recovered, which is discussed in De Vries et al. (2023b). The lower bound approximation forms the basis of the probabilistic background for the proof load testing method in the MBE (AASHTO, 2018), as described by Lichtenstein (1993).

2.3 Distribution of the resistance ratio (X)

A relation between indicator values and the resistance ratio, random variable X in Equations (2), may be deduced from the laboratory tests. Therefore, the laboratory measurements are post-processed to determine the resistance ratio for each load step. The maximum indicator value observed up to each load step is used instead of the actual indicator value for each load step. This approach mitigates the noise and erratic response in the crack-forming process. When specimens have failed the ratio is 1, reflecting that the resistance is at least equal to the current load effect but not higher (Figure 1, point 1). Once the ratios X_i from the laboratory test are obtained for each chosen indicator value, the data points may be analysed using the established knowledge of sample testing, e.g. Annex D of EN 1990 (CEN, 2019). Student's t-distribution is used to account for the typically small number of tests (Gosset, 1908). Of use here is the so-called *prediction distribution* for an assumed normally distributed population (Geisser, 1993):

$$X_{n+1} = M + TS\sqrt{1 + \frac{1}{n}} \tag{5}$$

where X_{n+1} is the next to-be-observed value, M is the sample mean, S is the sample standard deviation, n is the number of samples and T follows Student's t-distribution with v = n - 1 degrees of freedom. The sample mean and standard deviation, including Bessel's correction (n-1), are obtained through the well-known statistical formulas (Wasserman, 2004). Because the prediction distribution of X is used, the actual variation is more significant than solely indicated by the standard deviation.

3 APPLICATION TO A REINFORCED CONCRETE SLAB BRIDGE

3.1 Description

To demonstrate how the proposed method would be applied in practice, the structural reliability of a reinforced concrete slab bridge is considered. The bridge is fictional but characterises typical Dutch slab bridges without shear reinforcement. Deep beams representing strips of such a slab were tested in the laboratory to determine the shear resistance (Figure 2). Because the bridge is fictional and no actual load test was performed, a load test result must be assumed. In reality, indicator values following from actual measurements would be used.

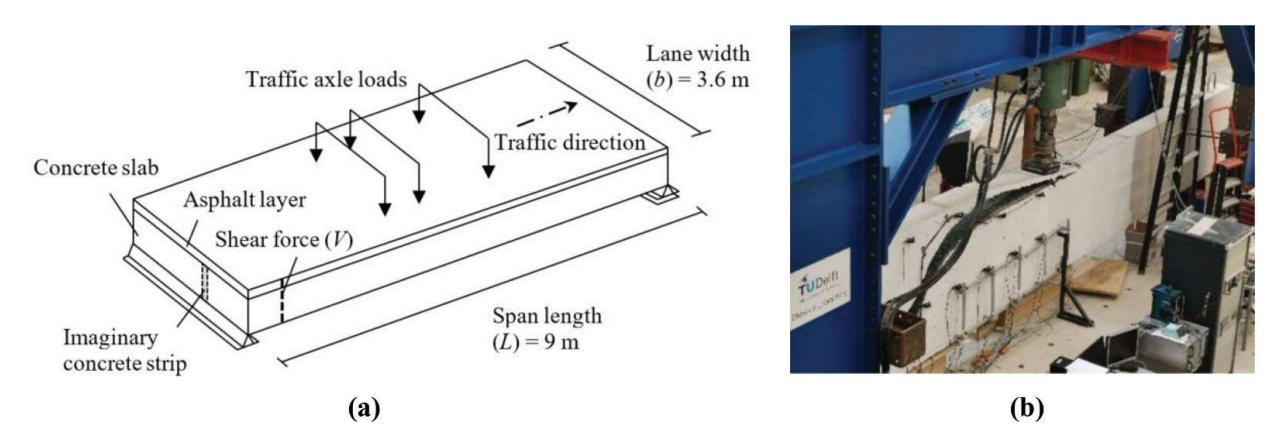


Figure 2. Reinforced concrete slab bridge considered in the case study, with (a) its schematic drawing and (b) a picture of one of the concrete strips tested to failure.

To simplify calculations only the first lane is considered, whilst in reality reinforced concrete slab bridges will typically have multiple lanes. The traffic load effect of the first lane is based on Weigh-In-Motion (WIM) measurements (FHWA, 2018) obtained from Dutch highways. The load effect in this case study is the shear force occurring at 1 m from the support (E = V). Loads applied at a smaller distance from the support are expected to travel directly to the support. For a span length of 9 m, the annual mean shear force is $m_Q = 390$ kN with a coefficient of variation $V_Q = 0.035$ (De Vries et al., 2023b).

The laboratory measurements used in this case study were initially designed to study the shear behaviour of reinforced concrete beams without shear reinforcement (Yang et al., 2021). The H-variants (H121, H401, H403, H404, H602) were used from the test series. These strips, or deep beams, had a height of 1.2 m and a width of 0.3 m. The simply supported beams were loaded by a single jack close to the middle of the span and resulted in shear failure close to the support. Given the assumed lane width, there are 3.6/0.3 = 12 strips within the considered slab.

3.2 Laboratory data post-processing

During the tests, Digital Image Correlation (DIC) was used to identify and follow the formation of cracks in the concrete (Jones & Iadicola, 2018). From the DIC results, the nominal crack width may be obtained for many locations (Gehri et al., 2020). The locations may be chosen arbitrarily, but DIC data must be available over the virtual gauge length. The gauge length that delivered the best results in this study was 0.8d, where d is the distance from the top of the beam to the middle of the longitudinal reinforcement. For each chosen location, the nominal crack width is calculated at the reinforcement level. In order to assign greater meaning to cracks forming near the supports, a weighted crack width is introduced where the nominal crack width is multiplied by the factor Vd/M where V and M are the shear force and bending moment at the considered location, respectively. Over the entire length of the beam, the maximum nominal crack width (w_{max}) and maximum weighted nominal crack width may be determined $(w_{\text{max,w}})$. The corresponding resistance ratio $X = V/V_{\text{u}}$ for both indicators was plotted for each load step (Figure 3).

The data was further post-processed to yield the sample mean and standard deviation for each considered indicator value (Figure 4). It is observed that the standard deviation of the data is smaller with the maximum weighted nominal crack width indicator ($w_{\text{max,w}}$), making it the best choice for further modelling. The data points with $w_{\text{max,w}} < 0.08$ mm result in very high mean and standard deviation values. This could result from noise in the DIC measurements for very small displacements. In general, the mean and standard deviation show some erratic behaviour considering different values of the indicator $w_{\text{max,w}}$. Therefore, an analytical model was fit to the result, which also describes the convergence towards reaching the true resistance with higher loads (Figure 4):

$$m_{V_{\rm u}/V}(w_{\rm max,w}) = \begin{cases} 1 + 1.6(w_{\rm max,w} - 0.85)^2 & w_{\rm max,w} < 0.85\\ 1 & w_{\rm max,w} 0.85 \end{cases}$$
(6a)

$$s_{V_{\rm u}/V}(w_{\rm max,w}) = \begin{cases} 0.3 - 0.3w_{\rm max,w} & w_{\rm max,w} < 1\\ 0 & w_{\rm max,w} 1 \end{cases}$$
 (6b)

A direct consequence of Equations (6a) and (6b), is that for $w_{\text{max,w}} \ge 1$ mm the method provides no benefit over proof load testing using the lower bound approximation (De Vries et al., 2023b).

3.3 Assumed load testing results

Section 3.1 describes the bridge under consideration as hypothetical and has not been tested in real life. However, an indication of reasonable indicator values is desired. The characteristic value

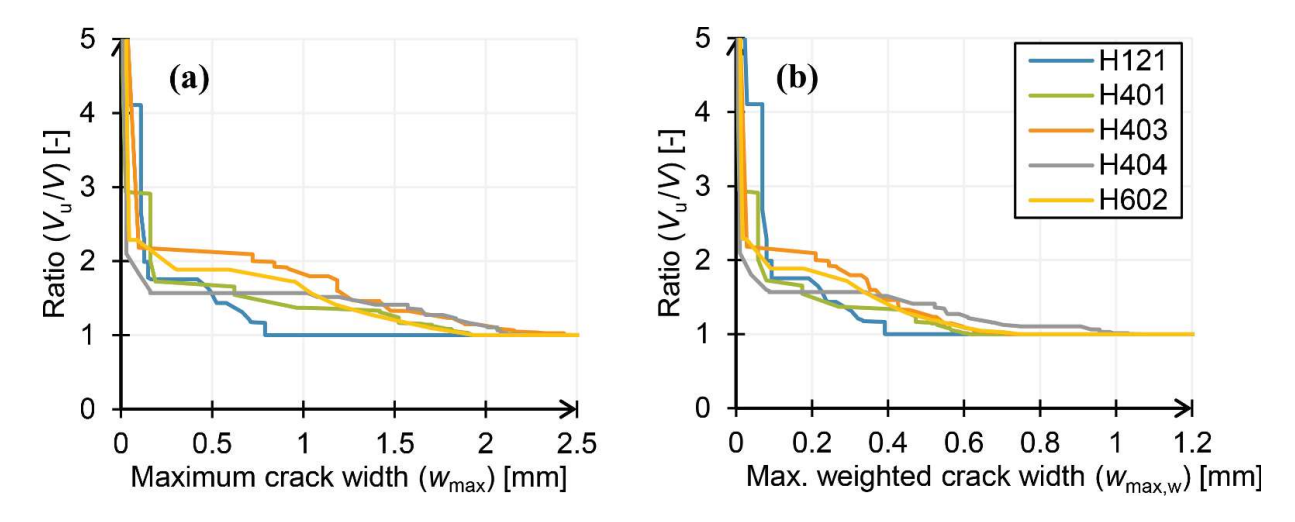


Figure 3. Shear resistance ratio versus (a) the maximum nominal crack width and (b) the maximum weighted nominal crack width.

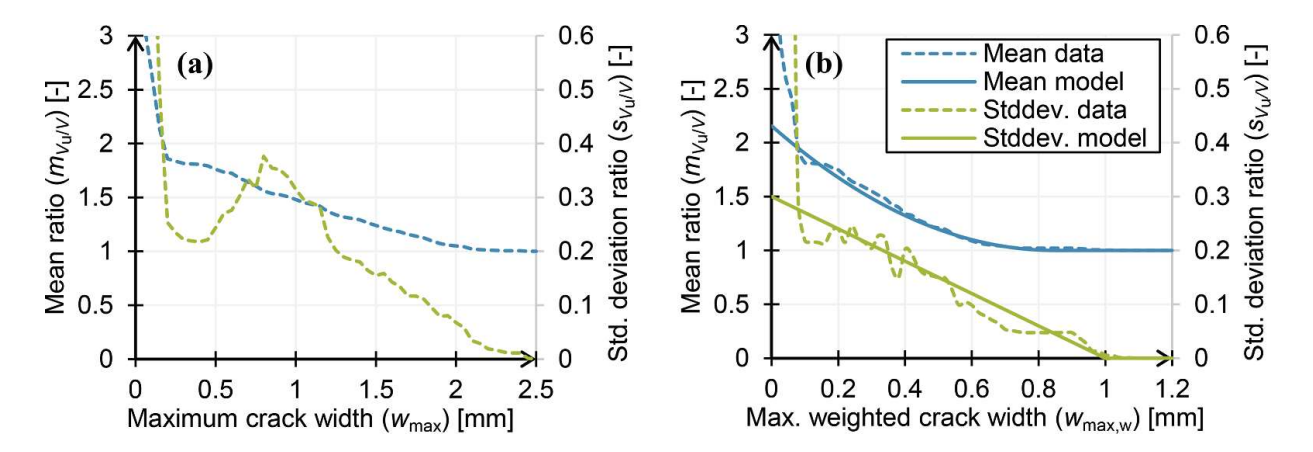


Figure 4. Mean and standard deviation of the shear resistance ratio versus (a) the maximum nominal crack width and (b) the maximum weighted nominal crack width.

of the traffic load multiplied by a factor serves as a helpful target load. Given the target loads, the laboratory test may provide reasonable indicator values (Table 1). When applied in practice, this step would not be necessary. The sensitivity to this input is described in the discussion (Section 5). It should be noted that the structure outside will already have the superimposed dead load ($G_{\rm SDL}$) included in the measurements – i.e. the starting point of the measurements is different. Therefore, the values in Table 1 for the case $G_{\rm DL}+G_{\rm SDL}$ should be added to the values obtained during field testing to relate them to the laboratory experiments.

Table 1. Expected indicator readings given proof load.

			Maximum crack width, weighted by position $(w_{\text{max,w}})$ [mm]					
Proof load test	Loadsacting on structure	Expected shear force [kN]	H121	H401	H403	H404	H602	Average
-	$G_{ m DL}$	30.0	0	0	0	0	0	0
-	G_{DL} + G_{SDL}	34.9	0.004	0.002	0.002	0.002	0.010	0.004
1	$G + Q_k$	73.0	0.069	0.058	0.019	0.010	0.016	0.034
2	$G + \tilde{1.2}Q_k$	80.6	0.069	0.058	0.023	0.010	0.029	0.038
3	$G + 1.4 \widetilde{Q}_{k}$	88.2	0.069	0.071	0.026	0.016	0.058	0.048
4	$G + 1.6\widetilde{Q}_{k}$	95.9	0.069	0.135	0.158	0.032	0.087	0.096

4 RESULTS

4.1 Probabilistic model

In this section, the case study of Section 3 is continued with reliability calculations following the method outlined in Section 2. Given the average indicator values from Table 1, the mean and standard deviation of the resistance ratio may be obtained from Equations (6a) and (6b), see Table 2. For each proof load test, a reliability analysis is performed using the random variables specified in Table 3. The mean and coefficient of variation are based on the Probabilistic Model Code (JCSS, 2015) and *fib* Bulletin 80 (fib, 2016). A small coefficient of variation (0.02) is used for model uncertainty of the resistance because the laboratory tests are assumed to be representative.

Table 2. Mean and standard deviation of the resistance ratio for each proof load test.

Proof load test	Mean PLeffect, strip $(m_{Q,PL,s})$ [kN]	Mean PLeffect, lane $(m_{Q,PL})$ [kN]	Indicator value $(w_{\text{max,w}})$ [mm]	Mean ratio $(m_{Vu/V})$ [-]	Std. deviation ratio $(s_{Vu/V})$ [-]
$1(Q_k)$	38.1	457.4	0.034	2.07	0.290
$2(1.2Q_{\rm k})$	45.7	548.8	0.038	2.06	0.289
$3(1.4Q_{\rm k})$	53.3	640.3	0.048	2.03	0.286
$4(1.6Q_{\rm k})$	61.0	731.8	0.096	1.91	0.271

4.2 Reliability calculation results

The annual reliability in the first year after the proof load test is calculated using the various limit state functions presented in Section 2 (assuming survival). In addition, the reliability is calculated using the lower bound approach that ignores permanent loads and additional resistance (i.e. X=1 and $\theta_R=1$). The calculations were performed with SORM (Hohenbichler et al., 1987), which approximately accounts for the non-linearity encountered in the limit state functions (Table 4). The results show that the calculated reliability indices are much higher compared to the lower bound approach. This reliability gain is the result of taking into account the measurements during proof load testing in the analysis (information source 2 in Figure 1). Even when the permanent loads are excluded from the limit state function, a target load of about $1.2Q_{k, WIM}$ would still be sufficient to satisfy annual $\beta=4$ requirement for CC3 (Steenbergen & Vrouwenvelder, 2010).

Table 3. Overview of random variables in the limit state function.

Var.	Description	Distribution	Mean	COV [-]
θ_R	Model uncertainty of the resistance	Lognormal	1	0.02
X	Resistance to current load effect ratio	Student's t, Equations (5)	(varies)	(varies)
$G_{ m DL}$	Dead load effect	Normal	356 kN	0.05
$G_{ m SDL}$	Superimposed dead load effect	Normal	59.3 kN	0.1
C_{0Q}	Time-invariant part of traffic load effect, including traffic trend	Lognormal	1.1	0.1
Q	Traffic load effect, annual maximum	Gumbel	390 kN	0.035
$\widetilde{Q}_{\mathrm{PL}}$	Load effect achieved by proof load	Normal	(varies)	0.02

Table 4. Mean and standard deviation of the resistance ratio for each proof load test.

		Annual reliability (β) [-]		
Characteristic load effect, WIM ($Q_{k,WIM}$) [kN]	Characteristic load effect, LM1 ($Q_{k,LM1}$) [kN]	Incl. permanent loads, Equations (3)	Excl. permanent loads, Equations (4)	Lower bound approach
1	0.78	3.21	3.02	0.70
1.2	0.93	4.11	4.02	2.31
1.4	1.09	5.03	5.00	3.66
1.6	1.24	5.86	5.85	4.78

5 DISCUSSION

In the laboratory data post-processing in Section 3.2, the model does not fit the data well for $w_{\text{max,w}} < 0.08$ mm. In the reliability calculations that follow, this region of minuscule cracks is used in the resistance prediction. Therefore, it may be questioned if the results can be trusted. Fortunately, as displayed in Figure 3, the data shows very high resistance ratios in this region with positive distribution skew. However, careful consideration must be made with regard to the similarity to the in-situ tested structure and the lab results. In the case study, it is assumed that the response of the bridge slab is similar to the response of the strips tested in the laboratory – presumably a conservative assumption, but it should still be validated.

An average response based on the laboratory measurements was assumed for the reliability calculations. In reality, the structure that is being tested may give a very different response and different measurement data post-processing may be necessary. When its strength is larger than expected and its condition is excellent, smaller indicator values are expected. When the assumed indicator values are divided by 10, the annual reliability indices increase by approximately 0.2. For structures that immediately display large crack widths under small loads, lower reliability is expected. When the indicator values are multiplied by 10, the reliability indices decrease by approximately 0.5 to 1. However, the reliability indices still remain higher than when calculated using the lower bound approach.

6 CONCLUSIONS

The proposed reliability updating method involves updating the resistance distribution using two sources of information: (1) the survival of the applied load in the proof load test and (2) the indicator value observed during the test, leading to an updated resistance distribution. A probabilistic model for updating the resistance distribution was presented, considering model uncertainties and permanent loads. The application of the proposed method was demonstrated through a case study of a reinforced concrete slab bridge. Laboratory data post-processing, including the consideration of weighted crack widths, provided insight into the resistance ratios considering different target loads. Reliability calculations based on the proposed method indicated a significant improvement compared to the lower bound approach, highlighting the importance of incorporating measured data.

The study addresses potential difficulties, particularly in fitting the model to data for small crack widths. It also recognizes the variability in real-world responses compared to assumed average values. Despite these considerations, the results consistently showed higher reliability indices than conservative estimates based on live loads alone. Real-world validation is recommended to enhance the robustness of the proposed approach. The next steps in the research will consider Bayesian approaches to include prior information in addition to the measurement data. Modelling choices and the application of the method with other types of resistance modes and measurements will be further reviewed.

REFERENCES

- AASHTO. (2018). The manual for bridge evaluation. Standard, 3rd Edition. Washington, D.C., USA.
- Alampalli, S., Frangopol, D. M., Grimson, J., Halling, M. W., Kosnik, D. E., Lantsoght, E. O. L., Yang, D. Y., & Zhou, E. (2021). Bridge Load Testing: State-of-the-Practice. *Journal of Bridge Engineering*, 26(3).
- Brüske, H. (2018). Structural test design with value of information. *PhD Thesis (Report 401)*, *DTU, Kongens Lyngby, Denmark*.
- CEN. (2019). Eurocode 0: Basis of structural design. In *Standard, EN 1990+A1+A1/C2:2019*. Brussels, Belgium: European Committee for Standardization.
- De Vries, R., Lantsoght, E. O. L., Steenbergen, R. D. J. M., & Fennis, S. A. A. M. (2023a). Time-dependent reliability assessment of existing concrete bridges with varying knowledge levels by proof load testing. *Structure and Infrastructure Engineering, In press*.
- De Vries, R., Lantsoght, E. O. L., Steenbergen, R. D. J. M., & Naaktgeboren, M. (2023b). Proof Load Testing Method by the American Association of State Highway and Transportation Officials and Suggestions for Improvement. *Transportation Research Record*.
- Faber, M. H., Val, D. V., & Stewart, M. G. (2000). Proof load testing for bridge assessment and upgrading. *Engineering Structures*, 22, 1677–1689.
- FHWA. (2018). Weigh-in-motion pocket guide Part 1: WIM technology, data acquisition, and procurement guide. Federal Highway Association, FHWA-PL-18-015, Washington D.C., USA.
- fib. (2016). Partial factor methods for existing concrete structures. Retrieved from Lausanne, Switzerland:
- Gehri, N., Mata-Falcón, J., & Kaufmann, W. (2020). Automated crack detection and measurement based on digital image correlation. *Construction and Building Materials*, 256.
- Geisser, S. (1993). Predictive inference: An introduction. New York: Chapman & Hall.
- Gosset, W. S. (1908). The probable error of a mean. *Biometrika*, 6(1), 1–25.
- Hohenbichler, M., Gollwitzer, S., W.,K., & Rackwitz, R. (1987). New light on first- and second-order reliability methods. *Structural Safety*, 4, 267–284.
- JCSS. (2015). Probabilistic model code. Retrieved from https://www.jcss-lc.org/jcss-probabilistic-model-code/.
- Jones, E. M., & Iadicola, M. A. (2018). *A good practices guide for digital image correlation*. Retrieved from https://doi.org/10.32720/idics/gpg.ed1/print.format
- Lantsoght, E. O. L., van der Veen, C., de Boer, A., & Hordijk, D. A. (2017). State-of-the-art on load testing of concrete bridges. *Engineering Structures*, *150*, 231–241.
- Lichtenstein, A. G. (1993). *Bridge rating through nondestructive load testing*. Retrieved from Washington, D.C., USA:
- Lin, T. S., & Nowak, A. S. (1984). Proof loading and structural reliability. *Reliability Engineering*, 8, 85–100.
- Steenbergen, R. D. J. M., & Vrouwenvelder, A. C. W. M. (2010). Safety philosophy for existing structures and partial factors for traffic loads on bridges. *Heron*, 55(2), 123–139.
- Wasserman, L. (2004). All of statistics: A concise course in statistical inference. *Book*, *Springer*.
- Yang, Y., Van der Ham, H. W. M., & Naaktgeboren, M. (2021). Shear capacity of RC slab structures with low reinforcement ratio An experimental approach. *fib Symposium*, *Lisbon*, *Portugal*.
- Zarate Garnica, G. I., & Lantsoght, E. O. L. (2021). Stop criteria for proof load testing of reinforced concrete structures. *Proceedings of the 2021 session of the 13th fib International PhD Symposium in Civil Engineering*, 195–202.